



# Pion production in p+p interactions and Be+Be collisions at the CERN SPS energies

Antoni Aduszkiewicz

*Institute of Experimental Physics, University of Warsaw*

*Antoni.Aduszkiewicz@fuw.edu.pl*

---

## Abstract

Evidence for the onset of deconfinement in central Pb+Pb collisions was reported by NA49 in fixed target measurements at beam momentum 30A GeV/c. This observation motivated the NA61/SHINE program started in 2009 at the CERN SPS, which, in particular, aims to study properties of the onset of deconfinement by measurements of hadron production in proton-proton, proton-nucleus and nucleus-nucleus collisions.

This contribution presents spectra of charged pions produced in p+p interactions and  ${}^7\text{Be}+{}^9\text{Be}$  collisions at 20A–158A GeV/c beam momentum. The NA61/SHINE results are compared with the corresponding NA49 data from central Pb+Pb collisions at the same beam momenta per nucleon.

*Keywords:*

---

## 1. Introduction

The NA61/SHINE experiment at the CERN SPS conducts a broad programme of hadron production measurement in proton-proton, nucleus-nucleus, proton-nucleus and pion-nucleus collisions. This paper focuses on measurements of collisions of protons and nuclei at different projectile momenta. A two-dimensional scan is performed in beam energy from 13A to 158A GeV/c and in system size from p+p up to Xe+La. It is planned to repeat and extend measurements of the NA49 experiment on Pb+Pb collisions [1, 2] with the upgraded NA61/SHINE setup. Figure 1 visualises the scan.

The scan aims to search for the critical point of the quark-gluon plasma phase transition and study the onset of deconfinement in collisions of light nuclei. The results presented in this paper relate to the latter topic.

This paper presents double differential spectra of negatively charged pions produced in p+p interactions at 20, 31, 40, 80 and 158 GeV/c (published [3]) and in  ${}^7\text{Be}+{}^9\text{Be}$  interactions at 40A, 75A and 150A GeV/c (preliminary), and positively charged pion spectra produced

in p+p interactions at 40, 80 and 158 GeV/c (preliminary).

## 2. Experimental set-up

### 2.1. Beams and targets

The experiment is located in the H2 beamline of the CERN North area. Secondary protons were selected with the desired beam momentum and directed on a 20 cm-long cell filled with liquid hydrogen served as the proton target.

The beryllium beam was produced by fragmentation of the primary Pb beam on a beryllium target. The H2 beam line was operated as a fragment separator. In order to ensure purity of the beam long-living  ${}^7\text{Be}$  nuclei were selected, as neighbouring isotopes:  ${}^6\text{Be}$  and  ${}^8\text{Be}$  are unstable and  ${}^{10}\text{Be}$  cannot be separated sufficiently from  ${}^9\text{Be}$ . The interaction target was made of stable  ${}^9\text{Be}$ .

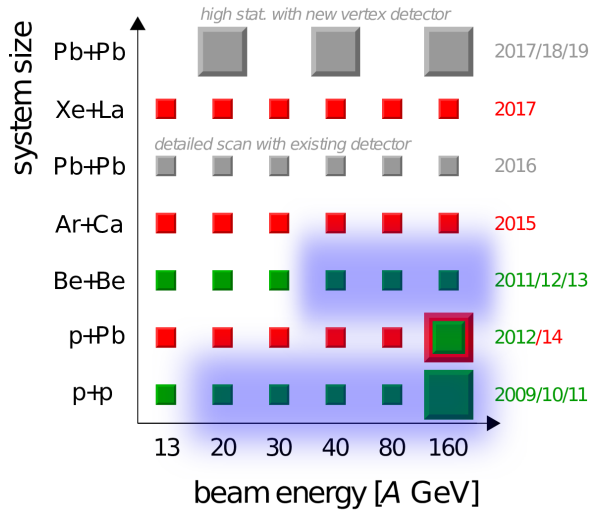


Figure 1: NA61/SHINE program of ion-ion collisions: two-dimensional scan in the system size (from p+p to Pb+Pb) and the projectile momentum (from 13A to 158A GeV/c). Each small box corresponds to 2–5 million of events; large boxes are 50 million. The green boxes show the data collected as of summer 2014, and the blue shade marks the data analysed in this paper.

## 2.2. NA61/SHINE detector

Figure 2 shows a schematic of the NA61/SHINE detector (upgrade of NA49 apparatus). Well-aligned beam particles are detected in a set of scintillation counters (S1, S2, V0, V1, V1'). An additional counter S4, used in anti-coincidence, was placed behind the target on the extrapolated beam trajectory. The beam is identified by two Cherenkov detectors: CEDAR and Threshold Cherenkov Counter (THC). The Be beam is also identified by the A detector (time of flight) and the Z detector (Cherenkov). The Projectile Spectator Detector (PSD) calorimeter on the extrapolated Be beam trajectory measures the non-interacting nucleons (spectators) of the projectile nuclei. Three Beam Position Detectors (BPD) measure the transverse coordinates of the interaction point. Produced charged particles are tracked in five Time Projection Chambers: two VTPCs placed inside magnets, two MTPCs and the GAP TPC. Time of Flight (ToF) walls are placed behind the MTPCs.

## 3. Analysis method

### 3.1. Derivation of spectra

The majority of the produced negatively charged hadrons are pions. A small (<10%) contribution of other hadrons, mostly  $\bar{p}$  and  $K^-$  can be reliably removed based on model predictions. This so-called  $h^-$  analysis

method allows to derive the  $\pi^-$  spectra in a broad phase-space region. The  $dE/dx$  identification method does not work at  $p < 4$  GeV/c where the Bethe-Bloch curves cross and at high momenta, where the statistics is insufficient to fit the data.

The  $h^-$  method was used to derive the  $\pi^-$  spectra in the full geometrical acceptance in p+p interactions at 20–158 GeV/c and in Be+Be collisions at 40–150A GeV/c. The  $dE/dx$  method was used to derive the  $\pi^-$  and  $\pi^+$  spectra in p+p interactions at 40–158 GeV/c in a more region. The results were corrected for the detector acceptance and efficiency and other experimental effects.

### 3.2. Centrality selection with PSD

Centrality of the  ${}^7\text{Be}+{}^9\text{Be}$  collisions was determined based on the forward energy measured with the PSD. Four centrality regions were defined: 0–5–10–15–25%.

Two effects shift the rapidity spectra in opposite directions:

- mass asymmetry between the projectile and the target biases the spectra towards negative rapidity,
- centrality selection with the PSD biases the spectra towards positive rapidity.

These effects cancel each other partially, however their impact on the results is still under investigation. For this reason only the mid-rapidity spectra will be discussed for Be+Be collisions.

## 4. Results

### 4.1. Double differential spectra

Double differential  $\pi$  spectra are shown in Figs. 3 and 4. The  $\pi^-$  spectra were derived with the  $h^-$  method in a large region of phase-space. The phase-space available for the  $\pi^+$  spectra obtained with the  $dE/dx$  method is the largest at 158 GeV/c. The missing region at low  $y$  and low  $p_T$  will be covered by the ToF analysis.

### 4.2. Comparison with the available data

Figure 5 shows integrated rapidity spectra of  $\pi^-$  and  $\pi^+$  mesons in p+p interactions. Within the systematic uncertainty the results of the  $h^-$  and the  $dE/dx$  methods agree. They also agree with the measurements of other experiments.

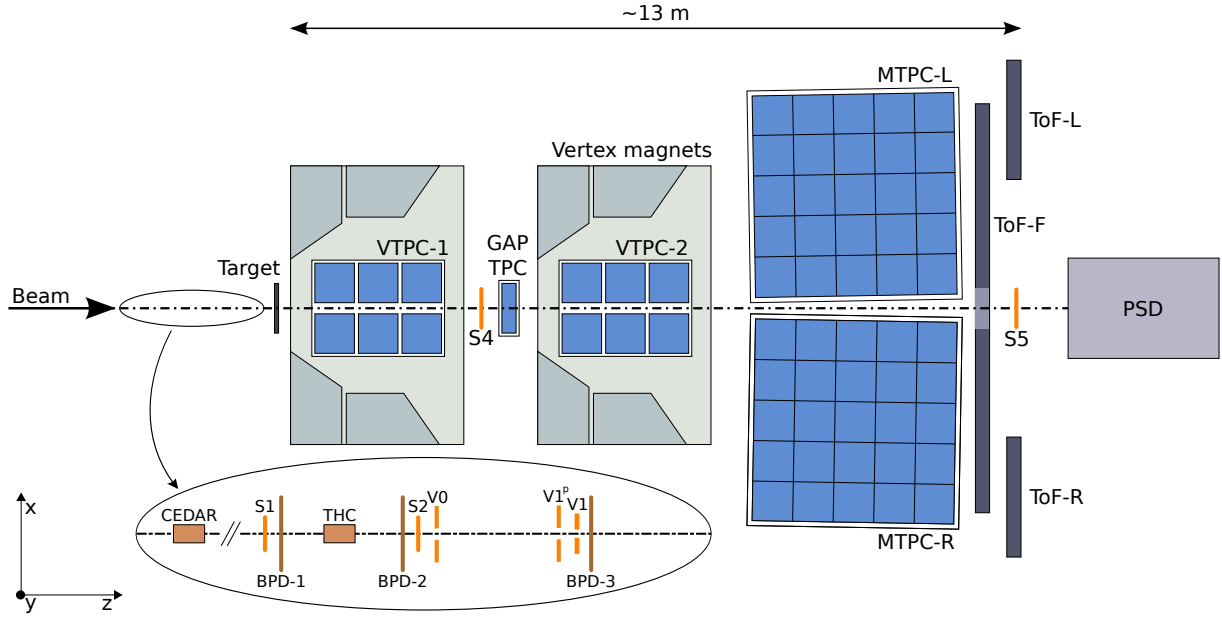


Figure 2: Schematic of the NA61/SHINE detector (horizontal cut, not to scale). The beam line set-up is magnified at the bottom of the figure. The spectrometer is formed by five Time Projection Chambers (TPC, blue). VTPCs are located inside VTX magnets. Behind the MTPCs there are three Time Of Flight (ToF) planes and the Projectile Spectator Detector (PSD) calorimeter.

#### 4.3. $\pi^-$ transverse mass spectra at mid-rapidity

The transverse mass ( $m_T = \sqrt{p_T^2 + m_\pi^2}$ ) spectra of  $\pi^-$  in p+p interactions and Be+Be collisions at 40A–150A GeV/c are shown in Fig. 6 (top). The spectra are fitted with an exponential function

$$\frac{1}{m_T} \frac{dn}{dm_T} = A \exp\left(-\frac{m_T}{T}\right) \quad (1)$$

in  $0.2 < m_T < 0.7$  GeV/c<sup>2</sup>. The fitted inverse slope parameter  $T$  is plotted against the number of wounded nucleons  $N_W$  (number of nucleons interacting inelastically) in Fig. 6 (bottom).  $T$  is seen to increase monotonically with  $N_W$ .

Figure 7 shows the energy dependence of the inverse slope parameter  $T$ . For Pb+Pb the  $T$  parameter is larger by 10–20 MeV than for p+p interactions. For Be+Be at 40A GeV/c  $T$  is the same as for p+p. At higher energies  $T$  increases by more than 10 MeV for Be+Be, while it is almost constant for p+p. This suggests the onset of collective effects for Be+Be collisions above 40A GeV/c.

Figure 8 shows the ratio of the transverse mass spectra of  $\pi^-$  mesons produced at mid-rapidity in central Pb+Pb collisions and inelastic p+p interactions at the same collision energy per nucleon. The spectra were normalised to unity before dividing. The ratio exceeds unity for  $m_T - m_\pi < 0.1$  GeV/c<sup>2</sup> and  $m_T - m_\pi >$

0.5 GeV/c<sup>2</sup>, while it is below unity in  $0.1 < m_T - m_\pi < 0.5$  GeV/c<sup>2</sup>, demonstrating different shapes of the spectra. The ratio shows weak dependence on the collision energy.

Comparison of p+p interactions and collisions of Pb nuclei, composed of protons and neutrons, requires taking into account the isospin symmetry. Full interpretation of the results requires  $\pi^+$  spectra in p+p derived in a large region of phase-space.

#### 4.4. $\pi^-$ rapidity spectra

Figure 9 shows the integrated rapidity spectra of  $\pi^-$ . The spectra are described well by the sum of two symmetrically displaced Gaussian distributions:

$$\frac{dn}{dy} = \frac{\langle \pi^- \rangle}{2\sigma_0 \sqrt{2\pi}} \cdot \left[ \exp\left(-\frac{(y-y_0)^2}{2\sigma_0^2}\right) + \exp\left(-\frac{(y+y_0)^2}{2\sigma_0^2}\right) \right], \quad (2)$$

Figure 10 shows the ratio of the  $\pi^-$  rapidity spectra normalised to unity in central Pb+Pb collisions and inelastic p+p interactions. Rapidity was normalised to beam rapidity  $y_{\text{beam}}$ . The distributions in Pb+Pb are broader as at  $y > 0.7$  the ratios exceed unity by 10–20%. The energy dependence is weak. Spectra of  $\pi^+$  in full phase-space are needed to understand the differences.

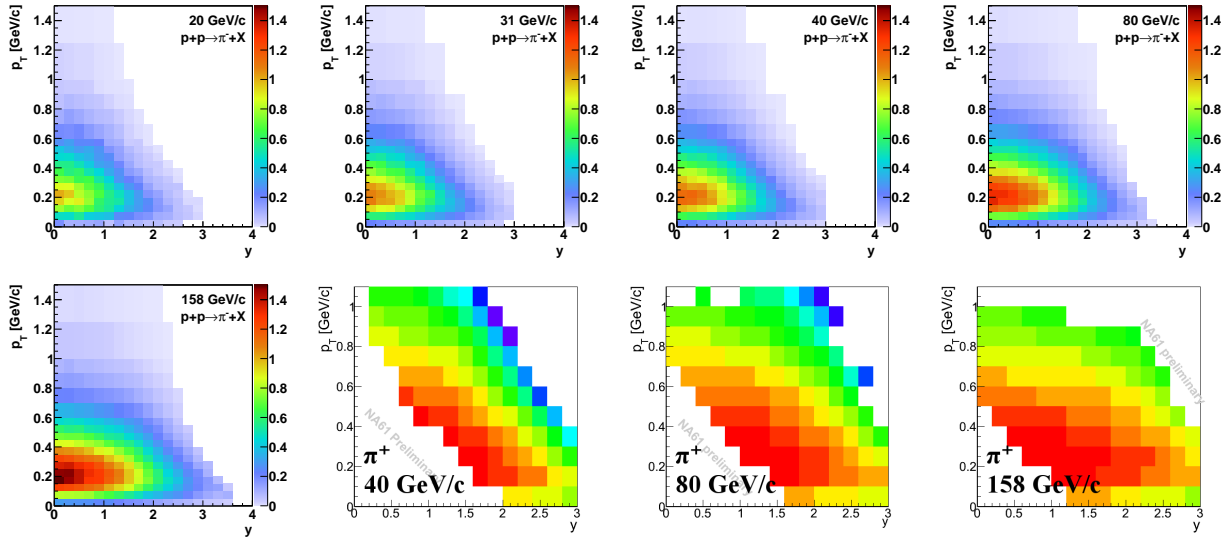


Figure 3: Double differential spectra  $\frac{d^2n}{dydp_T}$  of  $\pi^-$  in p+p interactions at 20, 31, 40, 80 and 158 GeV/c (first and second row) and  $\pi^+$  spectra in p+p interactions at 40, 80 and 158 GeV/c (second row).

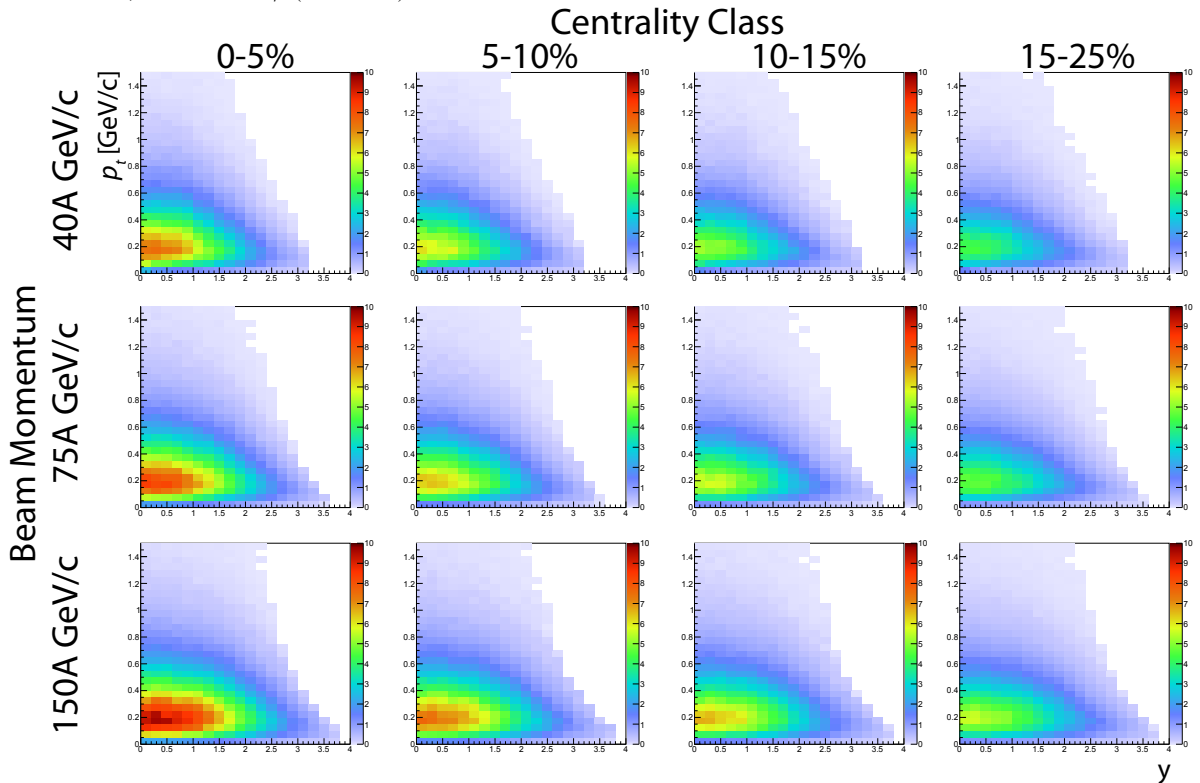


Figure 4: Double differential spectra  $\frac{d^2n}{dydp_T}$  of  $\pi^-$  in  ${}^7\text{Be}+{}^9\text{Be}$  collisions at 40A, 75A and 150A GeV/c in four centrality classes.

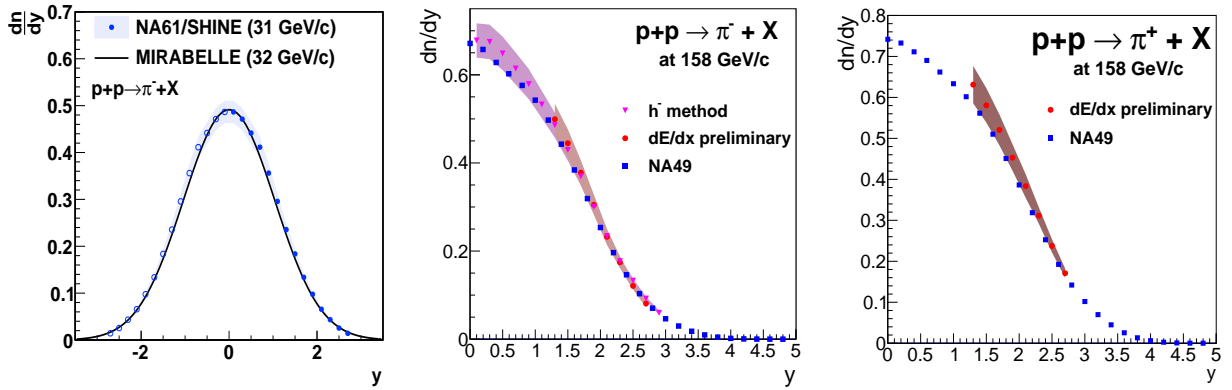


Figure 5: The NA61/SHINE integrated rapidity spectra of  $\pi^-$  and  $\pi^+$  mesons in inelastic p+p interactions at 31 and 158 GeV/c obtained with the  $h^-$  (left, middle) and dE/dx methods (middle, right), compared with results from MIRABELLE at 32 GeV/c [4] and NA49 at 158 GeV/c [5]. The shaded bands show the systematic uncertainty of the NA61/SHINE data.

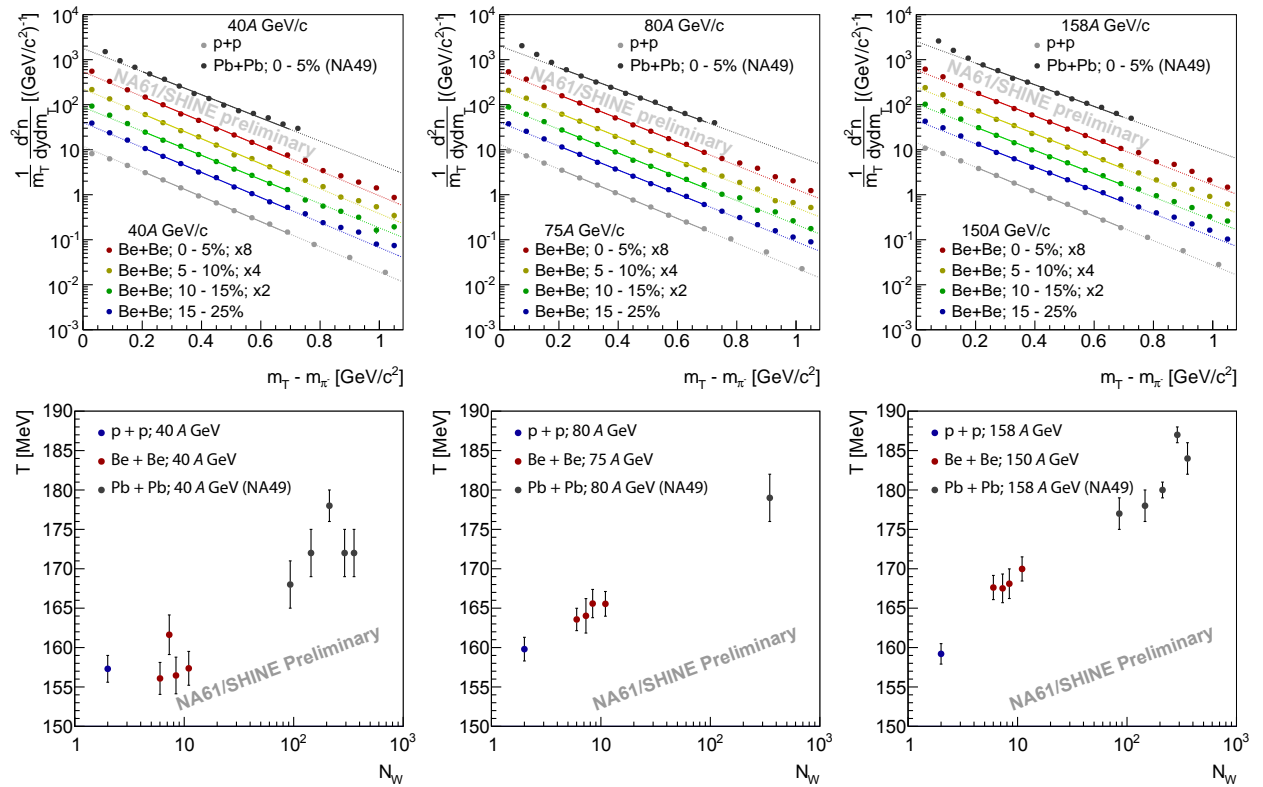


Figure 6: *Top*:  $\pi^-$  transverse mass spectra at mid-rapidity ( $0 < y < 0.2$ ) for inelastic p+p interactions, Be+Be collisions in four centrality regions and central Pb+Pb collisions [1] at 40A (left), 75/80A (middle) and 150/158A GeV/c (right). The spectra are fitted with an exponential function Eq. (1) in the regions of  $0.2 < m_T < 0.7$  GeV/c<sup>2</sup>, shown by thick solid lines. *Bottom*: fitted values of the inverse slope parameter  $T$  as a function of the number of wounded nucleons  $N_W$  for inelastic p+p interactions and Be+Be and Pb+Pb collisions.

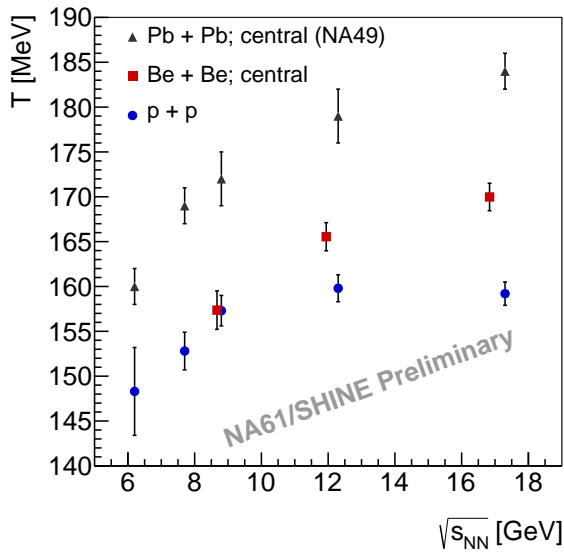


Figure 7: Inverse slope parameter  $T$  of the  $\pi^-$  transverse mass distributions in inelastic p+p and central Be+Be and Pb+Pb [1, 2] collisions. The  $T$  parameter was fitted in the region of  $0.2 < m_T < 0.7 \text{ GeV}/c^2$ .

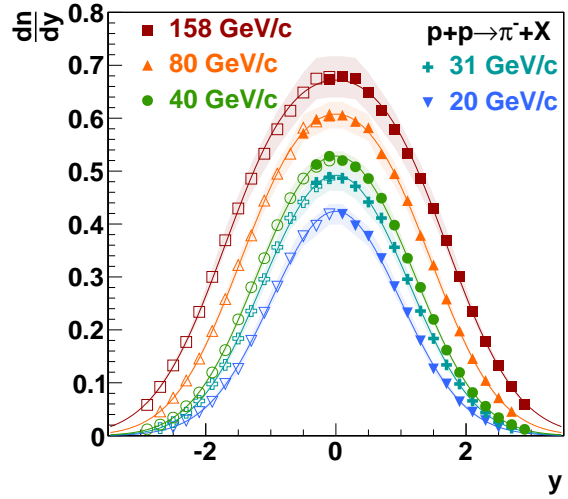


Figure 9: Integrated rapidity spectra of  $\pi^-$  produced in inelastic p+p interactions at 20–158 GeV/c. The open points are reflected with respect to  $y = 0$ . The shaded bands show the systematic uncertainty. The curves show function Eq. (2) fitted to the data.

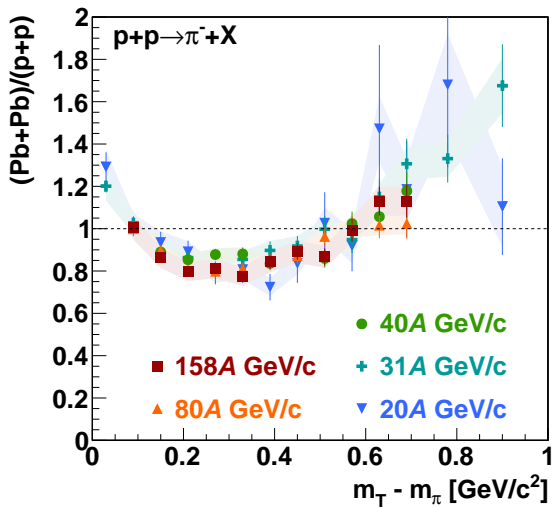


Figure 8: Ratio of the normalised  $\pi^-$  transverse mass spectra at mid-rapidity produced in central Pb+Pb collisions [1, 2] and inelastic p+p interactions at the same collision energy per nucleon. The coloured bands represent the systematic uncertainty of the p+p data.

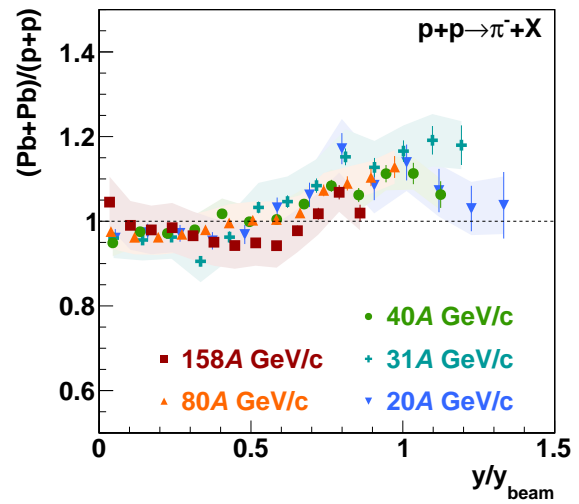


Figure 10: Ratio of normalised  $\pi^-$  integrated rapidity spectra of  $\pi^-$  in central Pb+Pb collisions [1, 2] and inelastic p+p interactions at 20A–158A GeV/c. The shaded bands show the systematic uncertainty of the p+p data.

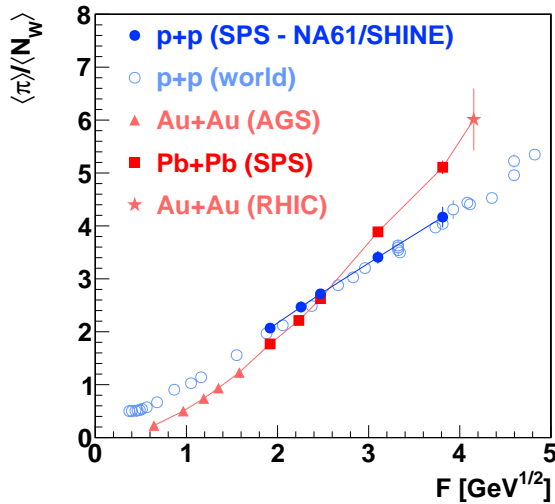


Figure 11: Mean multiplicity of all pions per wounded nucleon produced in inelastic p+p interactions and central Pb+Pb [1, 2] (Au+Au [6, 7, 8]) collisions versus Fermi energy  $F \approx s^{1/4}$  [9]. The vertical lines show the total uncertainty. The open points show results from the other experiments, mostly using bubble chambers [5, 10].

#### 4.5. Total pion multiplicity

The total  $\pi^-$  multiplicity was calculated by integrating the rapidity spectra. Known phenomenological relations between multiplicities of  $\pi$  of different charges [11] allowed to calculate the multiplicity of  $\pi$  of all charges. Figure 11 shows the energy dependence of the pion multiplicity  $\langle \pi \rangle$  divided by the number of wounded nucleons in inelastic p+p and central Pb+Pb collisions. The NA61/SHINE p+p results agree with results from other experiments. The multiplicity increases linearly with the Fermi energy  $F$  for p+p interactions. For central Pb+Pb collisions the increase is faster in the SPS energy region. This supported the conclusion that the onset of deconfinement in central Pb+Pb collisions occurs near 30A GeV/c [2]. The NA61/SHINE results demonstrate the capability of the experiment to study the onset of deconfinement in light ion collisions.

### 5. Conclusions

This paper presents the  $\pi^-$  spectra in full phase-space in p+p interactions at 20–158 GeV/c and in  ${}^7\text{Be}+{}^9\text{Be}$  collisions at 40A–150A GeV/c, as well as  $\pi^+$  spectra in limited phase-space in p+p interactions at 40–158 GeV/c. The results contribute to the NA61/SHINE programme of study of onset of deconfinement.

The inverse slope of the  $\pi^-$  transverse mass distribution in Be+Be collisions increases with energy above

40A GeV/c, while it is almost constant in p+p. This suggests the onset of collective effects in Be+Be collisions above 40A GeV/c. Spectra of  $\pi^-$  in p+p interactions and in central Pb+Pb collisions differ significantly.

Full interpretation of the presented results requires further investigation of the forward–backward asymmetry in Be+Be collisions. Spectra of  $\pi^+$  in full phase-space are required to understand the role of isospin effects.

### 6. Acknowledgements

Project financed by Narodowe Centrum Nauki based on decision DEC-2012/05/N/ST2/02759, Europejski Fundusz Społeczny and the State Budget under “Zintegrowany Program Operacyjnego Rozwoju Regionalnego”, Działania 2.6 “Regionalne Strategie Innowacyjne i transfer wiedzy” project of Mazowieckie voivodship “Mazowieckie Stypendium Doktoranckie”.

### References

- [1] S.V. Afanasiev *et al.* (The NA49 Collaboration), Energy dependence of pion and kaon production in central Pb+Pb collisions, *Phys. Rev. C* 66 (2002) 054902.
- [2] C. Alt *et al.* (The NA49 Collaboration), Pion and kaon production in central Pb+Pb collisions at 20A and 30A GeV: Evidence for the onset of deconfinement, *Phys. Rev. C* 77 (2008) 024903.
- [3] N. Abgrall *et al.* (The NA61/SHINE Collaboration), Measurement of negatively charged pion spectra in inelastic p+p interactions at  $p_{\text{lab}} = 20, 31, 40, 80$  and 158 GeV/c, *Eur. Phys. J. C* 74 (3) (2014) 2794, numerical results: <https://edms.cern.ch/document/1314605>.
- [4] E.E. Zabrodin *et al.*, Inclusive spectra of charged particles in pp and  $\bar{p}p$  interactions at 32 GeV/c, *Phys. Rev. D* 52 (1995) 1316.
- [5] C. Alt *et al.* (The NA49 Collaboration), Inclusive production of charged pions in p+p collisions at 158 GeV/c beam momentum, *Eur. Phys. J. C* 45 (2006) 343.
- [6] J.L. Klay *et al.* (E895 Collaboration), Charged pion production in 2A to 8A GeV central Au+Au Collisions, *Phys. Rev. C* 68 (2003) 054905.
- [7] L. Ahle *et al.* (E-802 Collaboration), Particle production at high baryon density in central Au+Au reactions at 11.6A GeV/c, *Phys. Rev. C* 57 (1998) R466.
- [8] B.B. Back *et al.* (PHOBOS Collaboration), Comparison of the total charged-particle multiplicity in high-energy heavy ion collisions with  $e^+e^-$  and pp/ $\bar{p}p$  data (2003). [arXiv: 0301017 \[nucl-ex\]](https://arxiv.org/abs/0301017).
- [9] E. Fermi, High energy nuclear events, *Prog. Theor. Phys.* 5 (4) (1950) 570.
- [10] M. Gaździcki, D. Roehrich, Pion multiplicity in nuclear collisions, *Z. Phys. C* 65 (1995) 215.
- [11] A. Golokhvastov, Koba–Nielsen–Olesen scaling in isospin-coupled reactions, *Phys. Atomic Nuclei* 64 (10) (2001) 1841.